

# Halogen-mediated exchange in the coupled-tetrahedra quantum spin systems $\text{Cu}_2\text{Te}_2\text{O}_5\text{X}_2$ ( $\text{X} = \text{Br}, \text{Cl}$ )

Roser Valentí,<sup>1</sup> T. Saha-Dasgupta,<sup>2</sup> Claudius Gros,<sup>1</sup> and H. Rosner<sup>3,\*</sup><sup>1</sup>Fakultät 7, Theoretische Physik, University of the Saarland, D-66041 Saarbrücken, Germany<sup>2</sup>S.N. Bose National Centre for Basic Sciences, JD Block, Sector 3, Salt Lake City, Kolkata 700098, India<sup>3</sup>Department of Physics, University of California, Davis, California 95616, USA

(Received 18 March 2003; published 26 June 2003)

Motivated by recent discussion on possible quantum critical behavior in the coupled Cu-tetrahedra system  $\text{Cu}_2\text{Te}_2\text{O}_5\text{Br}_2$ , we present a comparative *ab initio* study of the electronic properties of  $\text{Cu}_2\text{Te}_2\text{O}_5\text{Br}_2$  and the isostructural  $\text{Cu}_2\text{Te}_2\text{O}_5\text{Cl}_2$ . A detailed investigation of the copper-copper interaction paths reveals that the halogen ions play an important role in the inter-tetrahedral couplings via  $X_4$  rings ( $\text{X} = \text{Br}, \text{Cl}$ ). We find that, contrary to initial indications, both systems show a similar electronic behavior with long range exchange paths mediated by the  $X_4$  rings.

DOI: 10.1103/PhysRevB.67.245110

PACS number(s): 75.30.Gw, 75.10.Jm, 78.30.-j

The recently discovered<sup>1</sup> spin-tetrahedral compounds  $\text{Cu}_2\text{Te}_2\text{O}_5\text{X}_2$  ( $\text{X} = \text{Cl}, \text{Br}$ ) open the possibility to study the interplay between localized many-body tetrahedral cluster excitations and intertetrahedral magnetic couplings leading to a quantum-phase transition with various possible ordered states.<sup>2</sup> Transitions to ordered states have been observed experimentally<sup>3</sup> in these compounds with  $T_N^{(\text{Br})} = 11.4$  K and  $T_N^{(\text{Cl})} = 18.2$  K. These phase transitions exhibit unusual magnetic-field dependencies which have been linked to the closeness to a quantum-critical point.<sup>3,4</sup> Unconventional Raman scattering has been found in the magnetic channel<sup>2,3</sup> and the occurrence of low-lying singlet excitations has been proposed<sup>1</sup> and observed by Raman together with a longitudinal magnon.<sup>4</sup>

The nature of the ordered states in  $\text{Cu}_2\text{Te}_2\text{O}_5\text{X}_2$  has not yet been definitely settled. There is some evidence for a Néel state from thermodynamic and susceptibility experiments, and  $\text{Cu}_2\text{Te}_2\text{O}_5\text{Br}_2$  has been proposed to be closer to a non-magnetic singlet state than  $\text{Cu}_2\text{Te}_2\text{O}_5\text{Cl}_2$ .<sup>4</sup> Thus, it is important to examine the microscopic behavior of both  $\text{Cu}_2\text{Te}_2\text{O}_5\text{Br}_2$  and  $\text{Cu}_2\text{Te}_2\text{O}_5\text{Cl}_2$  by *ab initio* methods and investigate whether the electronic properties reveal some nontrivial differences between the two systems. The magnetic exchange coupling parameters in these systems estimated from susceptibility measurements<sup>1</sup> are small, of the order 40–50 K, implying a small bandwidth for the electronically active Cu  $3d$  orbitals close to the Fermi edge. Here we present a comprehensive first-principles density functional theory (DFT) study of the electronic properties of these systems within the local spin density (LSDA) and the generalized gradient approximation (GGA).<sup>5</sup>

## CRYSTAL STRUCTURE

Both  $\text{Cu}_2\text{Te}_2\text{O}_5\text{Br}_2$  and  $\text{Cu}_2\text{Te}_2\text{O}_5\text{Cl}_2$  systems crystallize in the noncentrosymmetric tetragonal  $P\bar{4}$  space group with two formula units per unit cell.  $\text{Cu}_2\text{Te}_2\text{O}_5\text{Br}_2$  with lattice parameters  $a = 7.84$  Å and  $c = 6.38$  Å has a larger unit cell than  $\text{Cu}_2\text{Te}_2\text{O}_5\text{Cl}_2$  with  $a = 7.62$  Å and  $c = 6.32$  Å.

In Fig. 1 we show the crystal structure for  $\text{Cu}_2\text{Te}_2\text{O}_5\text{X}_2$ .

The four equivalent  $\text{Cu}^{2+}$  ions in the unit cell of these systems form distorted tetrahedra which are located on a tetragonal lattice. The structure contains three inequivalent oxygen positions: the intratetrahedral O1, and the intertetrahedral O2 and O3. Of special interest are the four equivalent halogen ions, X, per unit cell which form together with the O1 and O2 the  $X\text{-O1-O1-O2}$  distorted square with the  $\text{Cu}^{2+}$  ions in their respective centers; see inset of Fig. 1. The intertetrahedron distances are slightly smaller in  $\text{Cu}_2\text{Te}_2\text{O}_5\text{Cl}_2$  than in  $\text{Cu}_2\text{Te}_2\text{O}_5\text{Br}_2$  due to the size difference of the respective halogen ions. The Cu-Cu intratetrahedron distances are, on the other hand, slightly larger in the Cl compound.

## BAND STRUCTURE

In Fig. 2 we present the non-spin-polarized band structure of  $\text{Cu}_2\text{Te}_2\text{O}_5\text{Br}_2$  and  $\text{Cu}_2\text{Te}_2\text{O}_5\text{Cl}_2$  near the Fermi level along various symmetry directions in the Brillouin zone. Calculations have been performed within the framework of the full potential linearized augmented plane wave (LAPW) method based on the WIEN97 code,<sup>6</sup> the full potential minimum basis local orbital code (FPLO),<sup>7</sup> and the linearized muffin tin orbital (LMTO) method based on the Stuttgart TBLMTO-47 code.<sup>8</sup> We compared the results obtained by the

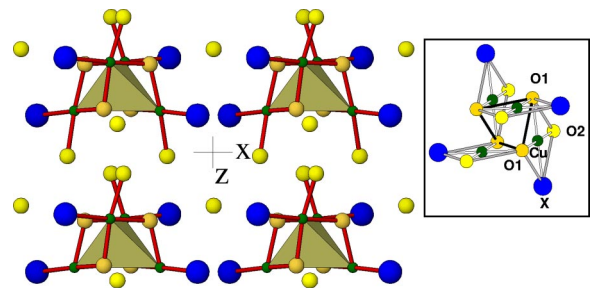


FIG. 1. Crystal structure of  $\text{Cu}_2\text{Te}_2\text{O}_5\text{X}_2$ . The small balls in the center of the bonds represent Cu, the medium sized and large balls O and the halogen X, respectively. The atom not connected to a bond is O3. For simplicity the Te atom was dropped. The inset presents an idealized  $\text{Cu}_4$  tetrahedron with the four corner-sharing O1-O1-O2-X idealized squares and the  $\text{Cu}^{2+}$  ion in the center.

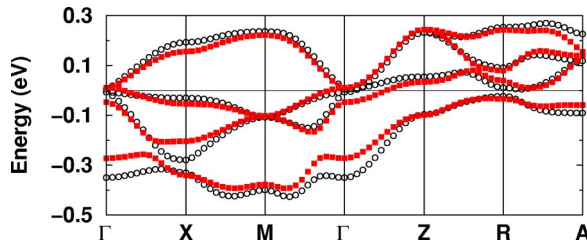


FIG. 2. Comparison of the LAPW band structure near the Fermi level between  $\text{Cu}_2\text{Te}_2\text{O}_5\text{Br}_2$  (full squares) and  $\text{Cu}_2\text{Te}_2\text{O}_5\text{Cl}_2$  (empty circles), with  $\Gamma=(0,0,0)$ ,  $X=(\pi,0,0)$ ,  $M=(\pi,\pi,0)$ ,  $Z=(0,0,\pi)$ ,  $R=(0,\pi,\pi)$  and  $A=(\pi,\pi,\pi)$ .

three methods in the GGA and the local density approximation (LDA). The band structures obtained by the three methods agree with each other within the allowed error bars of the various approximations involved in three different methods. The average error is seen to be of 0.02 eV. Here we present the energy bands, density of states, and electron density calculated with LAPW in the GGA approximation.

The four narrow bands of width  $\sim 0.7$  eV are well separated from the occupied low-lying valence band by a gap of  $\sim 0.25$  eV and the high-lying unoccupied Te  $p$  bands by a gap of  $\sim 2$  eV. The bands near the Fermi level do not contain essentially any Te orbitals. They are of dominant Cu  $3d$  character (predominantly  $3d_{x^2-y^2}$  in the local frame of reference), as shown in the partial density of states (DOS) in Fig. 3 with substantial admixture with Br(Cl)  $p$ , O1 and O2  $p$  states as shown in Fig. 4.

We can investigate these results further by analyzing the electron density. In Fig. 5 we present the electron density for  $\text{Cu}_2\text{Te}_2\text{O}_5\text{Br}_2$  for one tetrahedral unit. The lobes of the Cu  $3d$  orbitals are oriented towards the nearest neighbor Br, O1, O1, and O2 ions, which form the distorted square surrounding of the Cu ion. The covalent bonding in between the Cu  $3d$  orbital and the respective halogen  $p$  and oxygen  $p$  orbitals leads to the admixture of halogen and oxygen character at the Fermi level, as seen in the respective DOS (Fig. 4).

Comparing the band structure of both compounds near the Fermi level (see Fig. 2) we note that the bands of both systems are quite similar and only differ in some details that will translate in quantitative differences in the behavior of

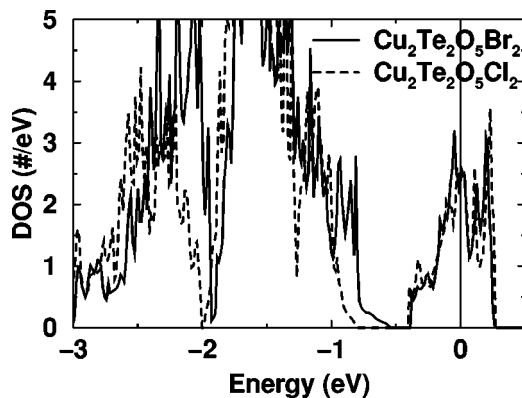


FIG. 3. LAPW density of states for the partial Cu  $3d$  orbitals.

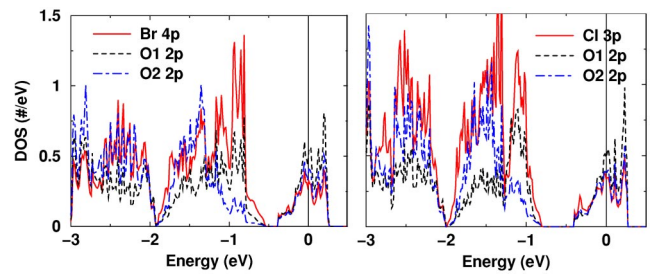


FIG. 4. LAPW density of states for the (total) halogen  $p$  and the O1  $p$  and the O2  $p$  orbitals, for  $\text{Cu}_2\text{Te}_2\text{O}_5\text{Br}_2$  (left) and  $\text{Cu}_2\text{Te}_2\text{O}_5\text{Cl}_2$  (right).

the effective model. The band dispersion, due to intertetrahedral matrix elements, is substantial (within the narrow bandwidth) along all three crystallographic directions indicating that the intertetrahedral couplings are nonnegligible in all three directions.

The DFT calculations yield, within the LDA or GGA approximation, to four half-filled (metallic) bands. We performed a spin polarized calculation which leads to an antiferromagnetic ground state in agreement with the experiment, although the resulting band gap of about 200 meV (about 50 meV for the ferromagnetic solution) is much too small. The antiferromagnetic spin arrangement led to a gain in total energy of about 240 meV (per Cu spin) compared to the fully ferromagnetically arranged Cu spins. For the antiferromagnetic ground state, the bandwidth of the antibonding bands was reduced by about 200 meV, whereas the bandwidth for the ferromagnetic state remained basically unchanged compared to the paramagnetic calculations. An additional local Coulomb repulsion—not taken fully into account in the LSDA or GGA approximation—will basically further shift these bands, enlarging the gap and resulting in the picture of lower- and upper-Hubbard bands in agreement with experiment. In the following, however, we did not do

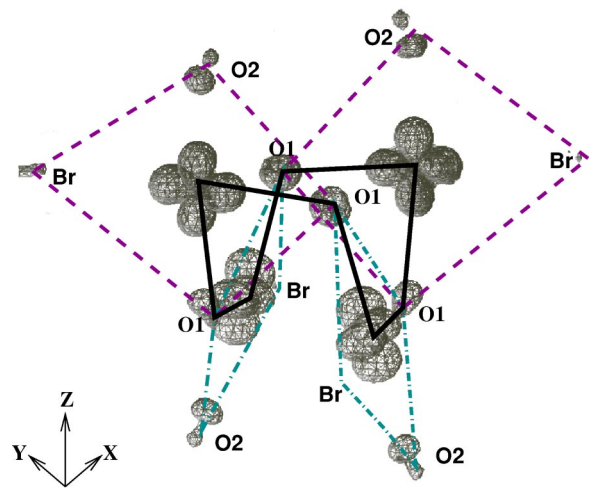


FIG. 5. LAPW electron density for  $\text{Cu}_2\text{Te}_2\text{O}_5\text{Br}_2$  at the 0.2 ( $e/\text{\AA}^3$ ) isovalue for one tetrahedron. The dashed and dashed-dotted lines indicate the four Br-O1-O1-O2 distorted squares with Cu placed in the respective centers; they share O1 corners. The solid line indicates the Cu-O1-Cu exchange paths ( $t_1$  in Fig. 6).

TABLE I. LMTO TB downfolding parameters for the effective Cu-Cu hoppings in meV units obtained by keeping active (i) the Cu  $3d$  orbitals (first and second columns, Cu downfolding) and (ii) both the Cu  $3d$  with the halogen  $3p/4p$  orbitals (third and fourth columns, Cu+X downfolding).

	Cu <sub>Br</sub>	Cu <sub>Cl</sub>		Cu+Br	Cu+Cl
$t_1$	80	98	$t_1$	155	181
$t_2$	4	0	$t_2$	-156	-132
$t_x$	-16	-10	$t_x$	-10	-14
$t_z$	11	12	$t_z$	34	33
$t_a$	-30	-29	$t_a$	5	8
$t_c$	-48	-45	$t_c$	-26	-19
$t_v$	-24	-23	$t_v$	9	8
$t_d$	-73	-80	$t_d$	8	8
$t_r$	-35	-48	$t_r$	-62	-72

the simulation of the missing Coulomb interaction in an LDA+ $U$  type calculation, which is in general useful but we do not expect from it new insights about the important couplings.

Attempts to directly compute the exchange integrals by comparing the LSDA total energy differences for different spin arrangements to that of a Heisenberg-like model faced two basic shortcomings: (i) The resulting magnetic moments at the copper sites were quite different for different spin arrangements. This leads to a strong bias of the interatomic exchange energies due to different intra-atomic contributions to the total energy. (ii) The important interactions in these compounds have a rather long-ranged nature as mentioned below. This would demand the calculation of large unit cells beyond the present computational capabilities. Therefore, we focus this letter to accessing the corresponding transfer integrals, thereby pointing out the important interaction pathways in these systems.

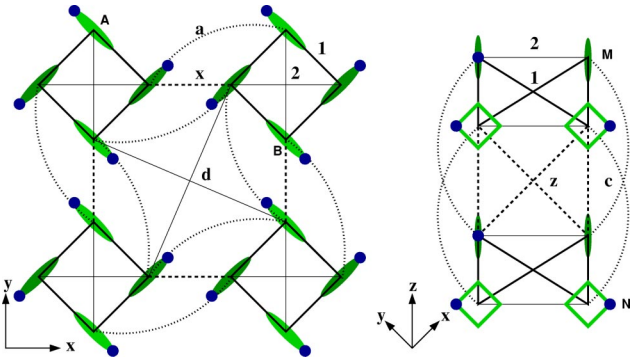


FIG. 6. Illustration of the hopping matrix elements  $t_\alpha$  ( $\alpha = 1, 2, x, z, a, c, d$ ) in between the  $\text{Cu}^{2+}$  ions which are located in the center of the  $\text{O}_3\text{X}$  distorted square ( $X = \text{Br}, \text{Cl}$ ), indicated by the shaded regions (not to scale, in reality the distorted squares share O1 corners). The filled circles denote the direction of the halogen sites. The parameters  $t_r$  and  $t_v$  correspond to the hopping elements between  $\text{Cu}^{2+}$  ions at A and B and at M and N, respectively, and equivalent positions.

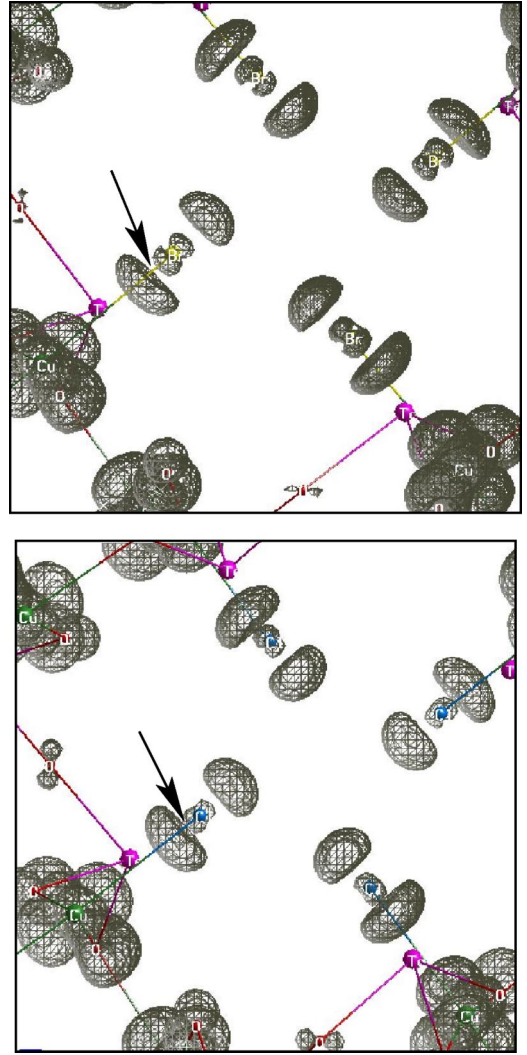


FIG. 7. LAPW electron density for  $\text{Cu}_2\text{Te}_2\text{O}_5\text{Br}_2$  (upper panel) and  $\text{Cu}_2\text{Te}_2\text{O}_5\text{Cl}_2$  (lower panel) at the  $0.05 (e/\text{\AA}^3)$  isovalue for a projection on the  $xy$  plane in between four Cu tetrahedra (compare with Fig. 6, left). The four  $p$  orbitals at the center are Br  $4p$  (upper panel) and Cl  $3p$  (lower panel). The respective arrows indicate the distortion of the  $X p$  orbitals.

## EFFECTIVE MODEL

In order to quantify the results obtained from the *ab initio* calculations in terms of hopping matrix elements,  $t_{ij}$ , we have employed LMTO-based downfolding<sup>9</sup> and tight-binding analysis on the band structure of these systems. The downfolding method implemented within the framework of the LMTO method consists in deriving a few-orbital effective Hamiltonian from the full LDA or GGA Hamiltonian by folding down the inactive orbitals in the tails of the active orbitals kept in the basis chosen to describe the low-energy physics of the system. This procedure naturally takes into account the proper renormalization effect of integrated-out inactive orbitals in the effective interactions defined in the basis of the active orbitals. Using the real-space description of the downfolded Hamiltonian one gets  $H_R = -\sum_{ij} t_{ij} (c_j^\dagger c_i + c_i^\dagger c_j)$ , where  $t_{ij}$  provides the effective hopping matrix elements between the active orbitals. In Table I we present the

results for the most significant hopping matrix elements—shown schematically in Fig. 6—obtained from downfolding the full LMTO Hamiltonian to effective Cu-only Hamiltonian by integrating out everything except the  $d_{x^2-y^2}$  orbital for each Cu atom in the unit cell to reproduce accurately the four narrow bands close to the Fermi energy. The first and second column of Table I show the hopping parameters for  $\text{Cu}_2\text{Te}_2\text{O}_5\text{Br}_2$  and  $\text{Cu}_2\text{Te}_2\text{O}_5\text{Cl}_2$ , respectively.

The predominant matrix elements consist of a set of nine different hopping parameters, some of them quite long-ranged and which could not be neglected in order to get a good description of the energy bands. Apart from the intratetrahedra  $t_1$  and  $t_2$  parameters, the intertetrahedra  $t_x$ ,  $t_z$ ,  $t_a$ ,  $t_c$ ,  $t_v$ ,  $t_d$  and  $t_r$  are important (see Fig. 6). For instance,  $t_c$  is needed in order to get dispersion along the path  $\Gamma-M$  and  $t_a$  and  $t_d$  are essential in order to get the correct behavior along the path  $X-A$ . The need of including such longer-ranged hoppings like  $t_r$  is set by the renormalization process of the downfolding procedure.<sup>10</sup> We note that long-ranged hopping matrix elements have proven to be essential for the description of some related copper systems.<sup>11</sup>

In order to investigate more in detail the nature of the Cu-Cu interaction paths and in particular the role of the halogen ion, we have also performed a tight-binding downfolding analysis of the bandstructure of both systems by keeping the halogen  $Xp$  orbitals active in addition to four Cu  $d$  orbitals in the basis set (Cu+ $X$  downfolding; see third and fourth columns of Table I). The results will be discussed in the following.

### INTRATETRAHEDRAL COUPLINGS

The nearest neighbor (NN) intratetrahedral Cu-Cu transfer matrix element  $t_1$  is mediated by O1 ions located in between two Cu ions and responsible for the Cu-O1-Cu superexchange generating the spin-spin coupling  $J_1$ . This superexchange path is shown in Fig. 5. The angle Cu-O1-Cu is  $107^\circ/109^\circ$  for  $X=\text{Br}/\text{Cl}$ . Assuming a similar crystal field, the larger superexchange angle for  $X=\text{Cl}$  results—following the Goodenough-Kanamori-Anderson rules<sup>12</sup>—in  $t_1(X=\text{Cl}) > t_1(X=\text{Br})$ , in agreement with the downfolding results; see Table I.

The intratetrahedral hopping matrix element  $t_2$  corresponds to the effective next nearest neighbor (NNN) Cu-Cu overlap. A comparison of the Cu- and the Cu+ $X$  downfolding result shows a substantial drop of  $t_2$  for both systems when the halogen-orbitals are integrated out. This drop indicates that paths of the type Cu- $X$ - $X$ -Cu are important for the effective  $t_2$  matrix element and that they compensate to a certain extent the contribution of the direct Cu-Cu path (see Fig. 5) and of other possible paths through oxygen ions. We note that  $t_2$  is vanishingly small in the Cl compound.

### INTERTEHEDRAL COUPLING

The coupling  $t_x$  via the O3 along the  $x$  and  $y$  directions in between two  $\text{Cu}_4$  tetrahedra (see Fig. 6 and Table I) is small, partly because the O3 weight is small at the Fermi level. There is, however, a substantial intertetrahedral coupling  $t_a$

and diagonal  $t_d$  within the  $xy$  plane mediated by the halogen  $p$  orbitals (see Figs. 6 and 7). The role of the halogen ions for the intertetrahedral couplings can be quantified by analyzing the Cu-downfolding and the Cu+ $X$ -downfolding results presented in Table I. Comparing the two corresponding values (Cu $_X$  and Cu+ $X$ ) we observe that  $t_a$  and  $t_d$  are nearly exclusively due to halogen-containing exchange paths.

The reason for this unusual large intertetrahedron coupling in  $\text{Cu}_2\text{Te}_2\text{O}_5\text{X}_2$  is the large extension of the Cl  $3p$  and Br  $4p$  wave functions which do not occur in cuprates containing only O  $2p$  orbitals (i.e.,  $\text{CuO}_4$  units). In contrast to certain other cuprate compounds containing halogen ions such as  $\text{Sr}_2\text{CuO}_2\text{Cl}_2$ ,<sup>13</sup> the situation for the  $\text{Cu}_2\text{Te}_2\text{O}_5\text{X}_2$  compounds is unique. Here, the halogen is part of the covalent Cu-O-Cl(Br) network, whereas in the former mentioned compound family the halogens play only the role of an anionic charge reservoir.<sup>13</sup>

A closer analysis of the electron density presented in Fig. 7 leads to two observations, which are in agreement with Cu+ $X$  downfolding results: (i) The Cl  $3p$  orbital at the Fermi level is more strongly distorted towards the Cu  $3d$  orbital compared to the Br  $4p$  orbital, indicating stronger copper-halogen coupling for  $X=\text{Cl}$  than for  $X=\text{Br}$  (see arrows in Fig. 7). (ii) The Br  $4p$  orbital is reoriented somewhat towards the NN Br  $4p$  orbital, indicating a stronger covalent Br-Br overlap. In addition to the intertetrahedral hopping processes along  $x$  and  $y$  there are substantial contributions to the intertetrahedral coupling terms  $t_c$ ,  $t_v$ , and  $t_z$  along the  $z$  direction; compare Fig. 6 and Table I.

### DISCUSSION

It has been recently argued<sup>4</sup> that  $\text{Cu}_2\text{Te}_2\text{O}_5\text{Br}_2$  and  $\text{Cu}_2\text{Te}_2\text{O}_5\text{Cl}_2$  differ only quantitatively but not qualitatively in their magnetic properties, with  $\text{Cu}_2\text{Te}_2\text{O}_5\text{Br}_2$  being somewhat closer to a quantum-critical phase transition. Here we present evidence from *ab initio* calculations that the electronic properties of these two compounds are indeed close and that the intertetrahedral coupling is considerable. We note that a substantial coupling between Cu tetrahedra is necessary in order to establish magnetic long-range order.<sup>4</sup>

We have also presented a detailed analysis in terms of two different downfolding models (Cu and Cu+ $X$ ) which reveal the important result that the halogen ions are essential for the intertetrahedral exchange couplings. We find that four halogen orbitals, coupled by considerable  $(X-p)-(X-p)$  covalent bonding, give rise to  $X_4$  rings which mediate long-ranged intertetrahedral couplings. These  $X_4$  rings are covalently coupled to the respective  $\text{Cu}_4$  tetrahedrons.

### ACKNOWLEDGMENTS

We acknowledge the support of the German Science Foundation (DFG SP1073) and discussions with F. Mila, P. Lemmens, and W. Brenig. We thank A. Kokalj for providing the graphics XCRYSDEN code.

- \*Present address: Max-Planck Institute for Chemical Physics of Solids, D-01187 Dresden, Germany.
- <sup>1</sup>M. Johnsson, K.W. Törnroos, F. Mila, and P. Millet, *Chem. Mater.* **12**, 2853 (2000).
- <sup>2</sup>W. Brenig and K.W. Becker, *Phys. Rev. B* **64**, 214413 (2001).
- <sup>3</sup>P. Lemmens, K.-Y. Choi, E.E. Kaul, C. Geibel, K. Becker, W. Brenig, R. Valentí, C. Gros, M. Johnsson, P. Millet, and F. Mila, *Phys. Rev. Lett.* **87**, 227201 (2001).
- <sup>4</sup>C. Gros, P. Lemmens, M. Vojta, R. Valentí, K.-Y. Choi, H. Kageyama, Z. Hiroi, N.V. Mushnikov, T. Goto, M. Johnsson, and P. Millet, *Phys. Rev. B* **67**, 174405 (2003).
- <sup>5</sup>J.P. Perdew, K. Burke, and M. Ernzerhof, *Phys. Rev. Lett.* **77**, 3865 (1996).
- <sup>6</sup>P. Blaha, K. Schwarz, and J. Luitz, *WIEN97: A Full Potential Linearized Augmented Plane Wave Package for Calculating Crystal Properties* (Karlheinz Schwarz, Technical Univ., Wien, Vienna, 1999).
- <sup>7</sup>K. Koepnick and H. Eschrig, *Phys. Rev. B* **59**, 1743 (1999).
- <sup>8</sup>O.K. Andersen, *Phys. Rev. B* **12**, 3060 (1975).
- <sup>9</sup>O.K. Andersen and T. Saha-Dasgupta, *Phys. Rev. B* **62**, R16219 (2000), and references therein.
- <sup>10</sup>We would like to mention here that a reduced set of hopping terms (i.e.,  $t_1$ ,  $t_2$ ,  $t_a$ ,  $t_d$ ,  $t_z$ ,  $t_x$ ) variationally varied to reproduce the behavior of the bands gives values for  $t_2$  comparable to  $t_1$  in the Br compound and values of  $t_d$  much smaller than those obtained with the larger set of parameters. This reduced set fails to reproduce accurately the bands—features along the path  $Z$ - $R$ - $A$ .
- <sup>11</sup>R. Valentí, T. Saha-Dasgupta, and C. Gros, *Phys. Rev. B* **66**, 054426 (2002); T. Saha-Dasgupta and R. Valentí, *Europhys. Lett.* **60**, 309 (2002).
- <sup>12</sup>J.B. Goodenough, *Phys. Rev.* **100**, 564 (1955); J. Kanamori, *J. Phys. Chem. Solids* **10**, 87 (1959); P.W. Anderson, *Solid State Phys.* **14**, 99 (1963).
- <sup>13</sup>R. Hayn, H. Rosner, V. Yu. Yushankhai, S. Haffner, C. Dürr, M. Knapfer, G. Krabbes, M.S. Golden, J. Fink, H. Eschrig, D.J. Singh, N.T. Hien, A.A. Menovsky, Ch. Jung, and G. Reichardt, *Phys. Rev. B* **60**, 645 (1999).